Remote Sensing of Environment 118 (2012) 40–49

Contents lists available at SciVerse ScienceDirect

Remote Sensing of Environment

journal homepage: www.elsevier.com/locate/rse

Relationship of a Landsat cumulative disturbance index to canopy nitrogen and forest structure

Lindsay N. Deel [a,*], Brenden E. McNeil [a], Philip G. Curtis [a], Shawn P. Serbin [b], Aditya Singh [b], Keith N. Eshleman [c], Philip A. Townsend [b]

[a] West Virginia University, Department of Geology and Geography, 98 Beechurst Avenue, 330 Brooks Hall, Morgantown, WV 26506-6300, USA
[b] University of Wisconsin – Madison, Department of Forest and Wildlife Ecology, 226 Russell Labs, 1630 Linden Drive, Madison, WI 53706-1598, USA
[c] University of Maryland Center for Environmental Science, Appalachian Laboratory, 301 Braddock Road, Frostburg, MD 21532, USA

ARTICLE INFO

Article history:
Received 21 January 2011
Received in revised form 25 October 2011
Accepted 29 October 2011
Available online 7 December 2011

Keywords:
Forest ecology
Disturbance
Landsat
Eastern forests
Ecosystem ecology
Disturbance index

ABSTRACT

Spatially-explicit knowledge of the timing, frequency, and intensity of forest disturbances is essential for forest management, yet little is known about how disturbances such as forest harvests and insect outbreaks might accumulate in their effects over time. Capturing the many forest harvest and insect defoliation events occurring over twenty-five years, we transformed a series of Landsat images into cumulative disturbance maps covering Green Ridge State Forest (GRSF) and Savage River State Forest (SRSF) in western Maryland. These maps summed yearly ΔDI images, which were defined as the change in a yearly tasseled cap disturbance index (DI), relative to a synthetic reference condition map created by finding the minimum DI value for all years. Intensive field-plot surveys and AVIRIS imagery collected during the summer of 2009 provided measurements of forest structure and canopy nitrogen. With these data, we found that while the most recent year's ΔDI had little relation, increases in the cumulative DI were related to decreased field-measured current canopy cover ($R^2 = 0.66$ at GRSF, 0.67 at SRSF and 0.34 combined) and watershed-averaged AVIRIS canopy N ($R^2 = 0.40$ at GRSF, 0.57 at SRSF and 0.54 combined). The latter relationship was obscured at the field-plot level of analysis, suggesting that fine scale studies will also need to account for other drivers (e.g. species composition) of variability in canopy N. Nevertheless, our study demonstrates that Landsat time series data can be synthesized into cumulative metrics incorporating multiple disturbance types, which help explain important cumulative disturbance-mediated changes in ecosystem functioning.

1. Introduction

Appalachian forests provide many ecosystem services, including carbon sequestration by taking in more atmospheric carbon dioxide (CO_2) during photosynthesis than they release during respiration. Similarly, the ability of a forest to retain nitrogen (N) from atmospheric deposition (e.g., acid rain) provides protection from acidification and eutrophication in streams and estuaries, processes that can endanger fisheries and human health (Driscoll et al., 2003; Likens, Bormann, Johnson, Fisher, & Pierce, 1970). These Appalachian forest ecosystem services are fundamentally linked to the canopy structure and concentration of N in canopy leaves (i.e., canopy N). Nitrogen is the major element limiting productivity in many terrestrial ecosystems (Vitousek & Howarth, 1991), including forests of the Eastern U.S. (LeBauer & Treseder, 2008). At the plant level, foliar N exerts a strong control over rates of photosynthesis (Evans, 1989; Wright et al., 2004), and of forest productivity and carbon sequestration at the canopy level (Ollinger et al., 2009; Pan, Hom, Jenkins, & Birdsey, 2004; Smith et al., 2002). Canopy N is also related to the ability of a forest to retain atmospheric N deposition (Aber et al., 1998), which has risen alongside atmospheric [CO_2] over the last century due to increased fossil fuel consumption and artificial fertilizer production (Galloway et al., 2008).

Remote sensing of canopy N through the use of hyperspectral instruments has greatly expanded the scale at which canopy N may be observed, enabling studies to be carried out across entire forested landscapes (Asner, 1998; Kokaly, 2001; Martin & Aber, 1997; Martin, Plourde, Ollinger, Smith, & McNeil, 2008; Ollinger & Smith, 2005; Ollinger et al., 2009; Wessman, Aber, Peterson, & Melillo, 1988). McNeil, de Beurs, Eshleman, Foster, and Townsend (2007) recently used these methodologies to link gypsy moth defoliation measured by MODIS with decreases in canopy N measured by NASA's Hyperion instrument.

While only recently explored with remote sensing (e.g., McNeil et al., 2007; Townsend, Eshleman, & Welcker, 2004), disturbances such as gypsy moth defoliation and logging are known to leave a marked ecological legacy, often manifested in the form of reduced nutrient availability (Eshleman, Morgan, Webb, Deviney, & Galloway,

* Corresponding author. Tel.: +1 757 814 1349.
E-mail address: ldeel@mix.wvu.edu (L.N. Deel).

0034-4257/$ – see front matter © 2011 Elsevier Inc. All rights reserved.
doi:10.1016/j.rse.2011.10.026

1998; Goodale & Aber, 2001; Latty, Canham, & Marks, 2004; Vitousek et al., 1979) and through reduced canopy cover (Bormann & Likens, 1979; Likens, Bormann, Pierce, & Reiners, 1978). Several recent studies have outlined implications of using past disturbance history in models of forest condition (e.g., Pan et al., 2011; Sader & Legaard, 2008). Indeed, most forests have a long disturbance history consisting of multiple disturbance events and land use changes; yet, there remains little understanding as to the cumulative effect of these disturbances on canopy N and forest structure.

Two of the disturbance types impacting eastern North American forests are gypsy moth defoliation and clear-cut harvesting. Gypsy moth (*Lymantria dispar*) defoliation represents an ongoing, ephemeral disturbance affecting eastern forests, with dominant outbreak periods occurring in approximately 8–10 year intervals and subdominant outbreaks in 5–6 year intervals (Haynes, Liebhold, & Johnson, 2009; Johnson, Liebhold, & Bjornstad, 2006). Evidence shows that plants may lose twice as much N through herbivory than they would through senescence (Chapin, Matson, & Mooney, 2002). Likewise, studies have shown dramatically altered forest structure, sustained nutrient losses, and shifts in species composition from clear-cut forests (Beck & Hooper, 1986; Likens et al., 1978; Vitousek & Reiners, 1975).

Several recent studies have successfully used the NIR and SWIR bands of the temporally rich Landsat dataset for mapping disturbance at the landscape scale (Cohen, Yang, & Kennedy, 2010; Jin & Sader, 2005; Kennedy, Cohen, & Schroeder, 2007; Kennedy, Yang, & Cohen, 2010). In particular, the disturbance index (Healey, Cohen, Zhiqiang, & Krankina, 2005) has been successfully used to map disturbances in a variety of forest types (DeRose, Long, & Ramsey, 2011; Eshleman, McNeil, & Townsend, 2009; Hais, Jonasova, Langhammer, & Kucera, 2009), including Appalachian forests. Substantial recent work has been focused on reconstructing past disturbance histories using Landsat time series with automated approaches that identify temporal trajectories of disturbance and recovery (Cohen et al., 2010; Goodwin, Coops, Wulder, & Gillanders, 2008; Huang et al., 2010; Kennedy et al., 2007, 2010; Thomas et al., 2011). A cumulative approach compliments such work by examining the additive influence of disturbance using stacks of Landsat data, thereby contributing insight on disturbance legacies in Eastern forests. Through the linkage of remotely sensed cumulative disturbance maps, such as from Landsat, to data on canopy nutrients we can develop a better understanding of long-term processes of nutrient dynamics. By examining the cumulative impacts of disturbances on forest ecosystems, we may gain insight into effective management strategies, and improve assessments of a variety of ecosystem services, such as carbon sequestration and nitrogen retention.

Our study sought to assess the cumulative impact of disturbance by analyzing the additive affects of multiple years of disturbance on forest dynamics. We explicitly addressed two major hypotheses about the relationship between canopy nitrogen, forest structure, and cumulative disturbance history: (1) as cumulative disturbance increases, we expected to see a subsequent decrease in canopy cover and (2) as cumulative disturbance increases, we expected to see a subsequent decrease in canopy N. Related to this, we postulated that past disturbances in a forest diminish over time in importance, yet still influence the current structure and nutrient status of a forest and that change maps of the current condition of a forest are not sufficient to explain patterns in the canopy structure and chemistry of that forest. Our study included analyses at the plot- (60 m radial) and watershed- (~0.8 km^2) scales.

2. Methods

2.1. Study areas

We conducted our research within two study areas: Green Ridge State Forest (GRSF) and Savage River State Forest (SRSF), both in western Maryland. These areas are delineated by the forest boundaries, but slightly expanded to include the complete hydrological unit codes (HUCs) at the HUC-11 level (Fig. 1). GRSF is in the warmer, dryer Ridge and Valley physiographic province in the rain shadow of the Allegheny Front and is dominated by oaks (Mash, 1996), while SRSF lies in the cooler, wetter Allegheny Plateau physiographic province and is dominated by northern hardwoods and oaks (Schaefer & Brown, 1991). Both areas experience considerable disturbance—including logging and gypsy moth defoliation, which typically occurs at 10–20 year intervals.

2.2. Field and laboratory methods

We sampled from a selection of existing plots that have been used in previous studies and supplemented with newly created sites for a total of twenty-eight 60-meter radial field plots within GRSF (18 plots) and SRSF (10 plots). These plots spanned the notable gradients of species types and disturbance histories (Table 1). To define the disturbance history gradients, we used ancillary data from personal accounts of state foresters, USDA sketch maps of gypsy moth defoliation (http://na.fs.fed.us/fhp/ta/av/) and Maryland Department of Natural Resources (DNR) maps of clear-cut timber harvests. Though the aerial sketch maps may have varying levels of quality due to different factors (e.g., different individual map creators), they have been used successfully in other studies to document historical defoliation patterns (e.g., Vogelmann, Tolk, & Zhu, 2009). We sampled plots representing six levels of historical disturbance identified using the ancillary data: not disturbed, harvested, harvested and defoliated, defoliated early (pre-1993), defoliated late (post-1993), and defoliated both early and late. We further divided the field plots into three major functional types (oaks, conifers, and northern hardwoods) in order to account for variability caused by species influences (Chapman, Langely, Hart, & Koch, 2006).

We collected all field data during July 2009 to maintain phenological consistency with the planned AVIRIS flights over GRSF and SRSF. Field data collection at the plot-level consisted of performing surveys using the point-quadrat camera method (Aber, 1979; MacArthur & Horn, 1969; Smith & Martin, 2001) to determine the fractional proportion of each species in the canopy and collecting species-specific green leaf samples for lab analysis of foliar chemistry, which ultimately allowed us to scale up canopy N values from the leaf level, then to the plot level, and finally, to the canopy level. We collected six estimates of canopy cover per plot using three different methods—densitometer readings, percent canopy cover estimates by cover

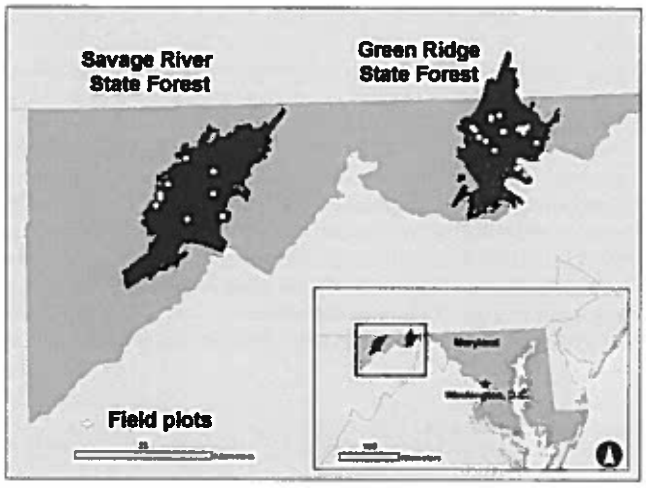

Fig. 1. Map of the study areas with field plots indicated by the white circles.

Table 1
Sample design matrix displaying number of plots sampled within each disturbance history and species type category. Disturbance histories are as follows: N.D. = not disturbed, H = harvested, D_e = defoliated early (pre-1991), D_r = defoliated recently (post-1991), $D_{e\&r}$ = defoliated both early and recently, and H & D = harvested and defoliated. N.H. refers to northern hardwood species.

	N.D.	H	D_e	D_r	$D_{e\&r}$	H & D
Oak	3	2	2	2	1	2
N.H.	1	2	3	2	1	3
Conifer	2	3	1	2	1	3

class, and percent canopy cover estimates by height—to provide information on forest structure.

In addition to performing plot surveys, we sampled individual trees representing dominant and subdominant species for fresh and dry leaf analysis of foliar chemistry. We pooled samples of individuals from high, medium, and low canopy heights by collecting small twigs using a pole pruner or shotgun with steel shot (McNeil et al., 2007; Smith & Martin, 2001; Townsend, Foster, Chastain, & Currie, 2003). We transported fresh leaf samples from the field to the laboratory at West Virginia University using Ziploc bags containing moist paper towels in a portable cooler to keep wet samples fresh (Garnier, Shipley, Roumet, & Laurent, 2001; Vaieretti, Diaz, Vile, & Garnier, 2007). We transported dry leaf samples from the field to the laboratory using paper bags.

Laboratory analysis of the field data involved two major components: the fresh analysis and the dry analysis. On the fresh leaves, we calculated leaf mass per area (LMA; g cm^{-2}) by measuring samples for fresh leaf mass (punching holes using a specified area for broadleaf species and scanning and calculating area for needleleaf species) and then drying and reweighing samples for dry leaf mass. The LMA measurements provided an essential element in the scaling of mass-based foliar N data from the leaf- to the plot-level. For the dry leaf analysis, we oven-dried all samples at 60 °C for 48 h and then ground them using a Willey Mill to pass through a 1-millimeter mesh screen. These ground leaf samples were then wrapped, weighed, and sent through a CNS analyzer to derive percent N values. We combined the LMA measurements and percent N values to calculate plot-level canopy N by using the mean species foliar N concentration per plot, weighted by fraction of canopy foliar mass per species at each plot (Smith & Martin, 2001).

2.3. Landsat methods

We took advantage of the temporal range of Landsat by using a total of 14 images (Table 2) spanning approximately twenty-five years ranging from 1984 until 2008 and generally covering the summer months (June–early September). Persistent cloud cover, common to the study areas, prevented the use of anniversary dates and images for every individual year up to the present. We applied a uniform mask to each of the images to remove nonforested areas and clouds. Even partial cloud cover resulted in a much larger masked area for all images, so we chose to exclude images with more than a few small clouds. We created the non-forest mask using the 2001 National Land Cover Dataset (NLCD) combined with a supervised classification. We implemented the COST method of atmospheric normalization (Chandler, Markham, & Helder, 2009; Chavez, 1996), which converts digital number (DN) values to reflectance values. We tested the imagery for terrain effects and found no relationship between illumination, determined using a hillshade of the study areas, and the cumulative disturbance index values ($r^2 = 0.0055$); therefore, we did not apply a terrain correction.

Healey et al. (2005) introduced the disturbance index (DI) as a Tasseled Cap-derived measure that can be used for forest disturbance detection. We normalized each Tasseled Cap band to image-specific z-scores, which partially accounts for phenological variation from image to image. The DI highlights the fact that disturbed areas tend to exhibit higher values of brightness (B) and lower values of greenness (G) and wetness (W) than undisturbed areas, resulting in high, positive DI values for recently disturbed areas; low, negative DI values for areas that have recently recovered from disturbance or experienced abnormally rapid growth; and all other forest pixels, assumed to be undisturbed, falling near zero (Healey et al., 2005; Fig. 2).

Table 2
Ancillary GIS data and Landsat imagery used for creation of the cumulative disturbance indices and subsequent analyses.

Data	Source and date
Timber harvest GIS shapefiles	Forest Managers at GRSF and SRSF (1969–2001)
Gypsy moth defoliation shapefiles	United States Forest Service (1984–2008)
Species composition maps	Foster and Townsend (2004) (2000)

Image date	Path	Row	Sensor	Study area
9/19/1984	16	32/33	Landsat TM 5	GRSF and SRSF
8/18/1987	17	32/33	Landsat TM 5	SRSF
8/03/1990	16	31/33	Landsat TM 5	GRSF
8/22/1991	16	32/33	Landsat TM 5	GRSF
6/24/1993	16	32/33	Landsat TM 5	GRSF and SRSF
6/09/1999	16	33	Landsat TM 5	SRSF
8/04/1999	16	32/33	Landsat ETM+	GRSF
8/22/2000	16	32/33	Landsat ETM+	GRSF
7/24/2001	16	32/33	Landsat ETM+	GRSF
8/12/2002	16	32/33	Landsat ETM+	GRSF
6/25/2005	16	32/33	Landsat TM 5	GRSF and SRSF
8/06/2006	17	32/33	Landsat TM 5	SRSF
8/25/2007	17	32/33	Landsat TM 5	SRSF
7/19/2008	16	32/33	Landsat TM 5	GRSF

One difficultly in addressing forest change detection is finding pixels within an image that can be called "undisturbed" with which to compare disturbed pixels. Rather than comparing DI values with one single previous or subsequent year, we compared each yearly DI image with a DI_{min} image, generated by taking the lowest, or 'least disturbed' DI value for each pixel from the stack of yearly DI images (Fig. 2). The DI_{min} is essentially a composite of all image dates, and it provides a snapshot of the forest in its least disturbed state (Fig. 3). This allowed us to more objectively assess the total change in DI from a relatively undisturbed state. The change detection between DI_{min} and the individual yearly DI images consisted of a simple image subtraction (Eq. (1); Fig. 2):

$$\Delta DI = DI - DI_{min} \quad (1)$$

Thus, the resulting ΔDI images represent the change experienced from the 'least disturbed' DI_{min} image to each study year. One advantage of estimating cumulative disturbance using our ΔDI images calculated using the DI_{min} is that they essentially remove the potentially confusing negative values associated with regrowth. By subtracting the minimum values (DI_{min}) from each DI image, the equation eliminates negative values, which generally correspond with regrowth. Thus, in the ΔDI images, the minimum value is never less than zero (Fig. 2).

In order to obtain a value of cumulative disturbance, we summed up all ΔDI images and applied an exponential weighting scheme (Malczewski, 1999) to the sum, attributing the highest weights to the most recent years and the lowest weights to the earliest years (Table 3; Fig. 4). While this exponential weighting scheme was the strongest of several other weighting schemes (e.g., linear) explored in our preliminary analysis, it should still be viewed as a working hypothesis quantifying how the impacts of disturbance are likely to decrease over time.

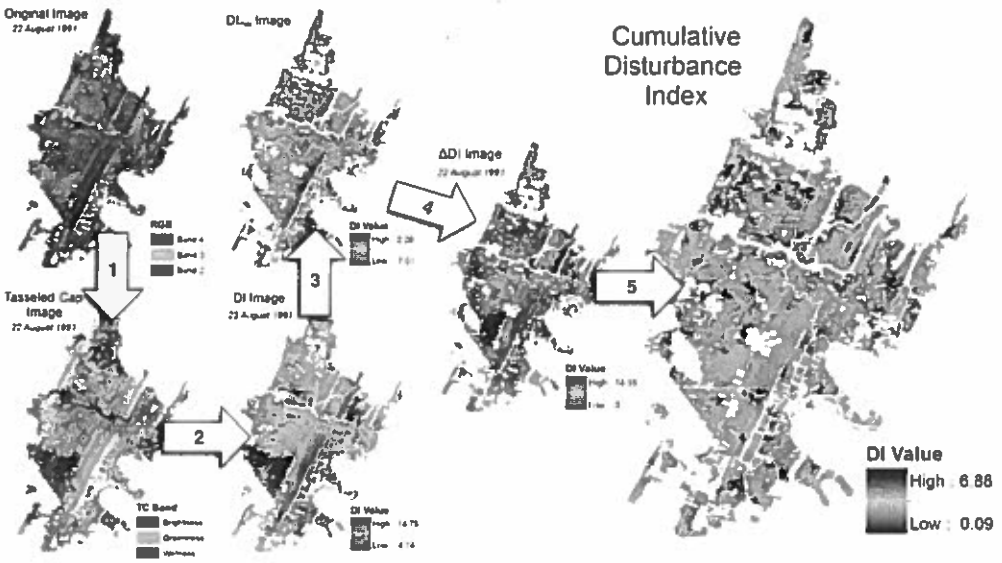

Fig. 2. Flowchart of the remote sensing methods used to create the cumulative disturbance index: 1) original image transformed using the tasseled cap transformation, 2) disturbance index (Healey et al., 2005) calculated using the normalized tasseled cap bands, 3) minimum DI values extracted from all images to create the DI_{min} image, 4) a change map, ΔDI, created for each year by subtracting the DI_{min}, and 5) the final cumulative DI image created by combining each ΔDI image in a weighted sum. Non-forested land cover and clouds are masked.

2.4. AVIRIS methods

NASA's ER2 aircraft – housing the Airborne Visible/Infrared Imaging Spectrometer (AVIRIS) instrument – acquired high spectral resolution imagery at 20 km altitude using two flights on July 6 and 14, 2009. The spatial resolution of the imagery is 17–20 m, and the spectral range of 374–2508 nm at 10-nm intervals covers 224 bands (Green et al., 1998). The flights corresponded with field data collection within the study areas during peak summer growing months. We acquired a total of four images over the study sites: two covering SRSF and two covering GRSF. After pre-processing, we followed the general methods of Martin et al. (2008) to create canopy N maps from the 2009 AVIRIS data.

Image preprocessing involved five distinct steps, including the development of an integrated cloud and cloud-shadow mask, cross-track illumination correction, removal of overlapping bands, correction of atmospheric effects and conversion to top-of-canopy (TOC) reflectance, and terrain illumination correction. After preprocessing, the images were left with 183 bands to be used in the partial least squares (PLS) regression equation.

We extracted reflectance spectra from the single nearest pixel to each field plot coordinate from both study sites and all four images, and then used PLS regression to relate field measurements of plot-level canopy N with the remaining 183 bands of reflectance spectra from the four AVIRIS images (Martin et al., 2008; Smith, Martin,

Fig. 3. The DI_{min} classified by the year of origin for each pixel. Non-forested land cover and clouds are masked.

Table 3
The weights used to calculate the cumulative disturbance index. Weights were calculated using the following equation: $(n-r_i+1)^P$, where n = the total number of years (25), r = the straight rank, and P = 2 (Malczewski, 1999).

Image year	Straight rank	Weights	Normalized
1984	25	1	0.000272183
1987	22	16	0.004354927
1990	19	49	0.013336962
1991	18	64	0.017419706
1993	16	100	0.027218291
1999	10	256	0.069678824
2000	9	289	0.07866086
2001	8	324	0.088187262
2002	7	361	0.098258029
2005	4	484	0.131736527
2006	3	529	0.143984758
2007	2	576	0.156777354
2008	1	625	0.170114317
	Sum	3674	1

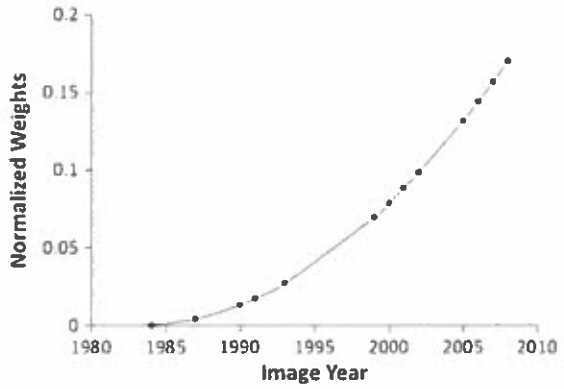

Fig. 4. The exponential weighting scheme used to create the cumulative disturbance index.

Ollinger, & Plourde, 2003; Smith et al., 2002). PLS allows for a regression analysis to relate a large number of independent variables to a much smaller number of dependent variables by reducing the independent variables into a specified number of latent factors. We used four latent factors in our model because this number of factors minimized the predicted residual sum of squares statistic (PRESS) given within the PLS analysis (Townsend et al., 2003). The PLS regression provided a set of regression coefficients and loadings for each band (Fig. 5). We then applied the regression coefficients to the imagery to generate the canopy N map (Fig. 6).

2.5. Statistical analyses

We used regression analyses to test whether increased cumulative disturbance was predictive of decreased forest canopy cover at the plot-scale and canopy N at the plot- and watershed-scales. For watershed-scale analyses, we used fifty-four first-order watersheds used in a previous study by Townsend et al. (2004) and in unpublished related work. In order to account for any slight difference in the plot locations and the image geometry, we ran a low pass filter over the cumulative disturbance images, which averaged pixels in a 3×3 moving window across the entire image. We used the filtered images to extract pixel values for statistical analysis. For comparison, we also tested this relationship against the most recent ΔDI image for each study area. This comparison allowed us to explore whether cumulative DI was more associated with the additive impacts of disturbance than only the most recent year of imagery.

3. Results

3.1. Cumulative disturbance index

The cumulative DI map displays values ranging from 0.09 to 6.88 at GRSF and from 0.03 to 8.05 at SRSF. The most recent ΔDI images display values ranging from 0 to 26.95 at GRSF and from 0 to 19.78 at SRSF. While the weighting scheme causes differences in their dynamic range, the cumulative DI and most recent ΔDI maps both represent relative disturbance intensities, with lower values representing less disturbance and higher values representing more disturbance. The maps of cumulative DI identify known patterns of clear-cut forest harvest and gypsy moth defoliation that occurred throughout the study period (Fig. 7). Forest harvest patterns were immediately evident, but cumulative DI was more variable within areas that foresters had marked as defoliated on the GIS sketch map ancillary data. These differences in the mapped spatial pattern of disturbances match our knowledge of these disturbance agents; harvested areas tend to be located in relatively discrete areas defined by forest management practices, while defoliations occur in varying intensities across the landscape.

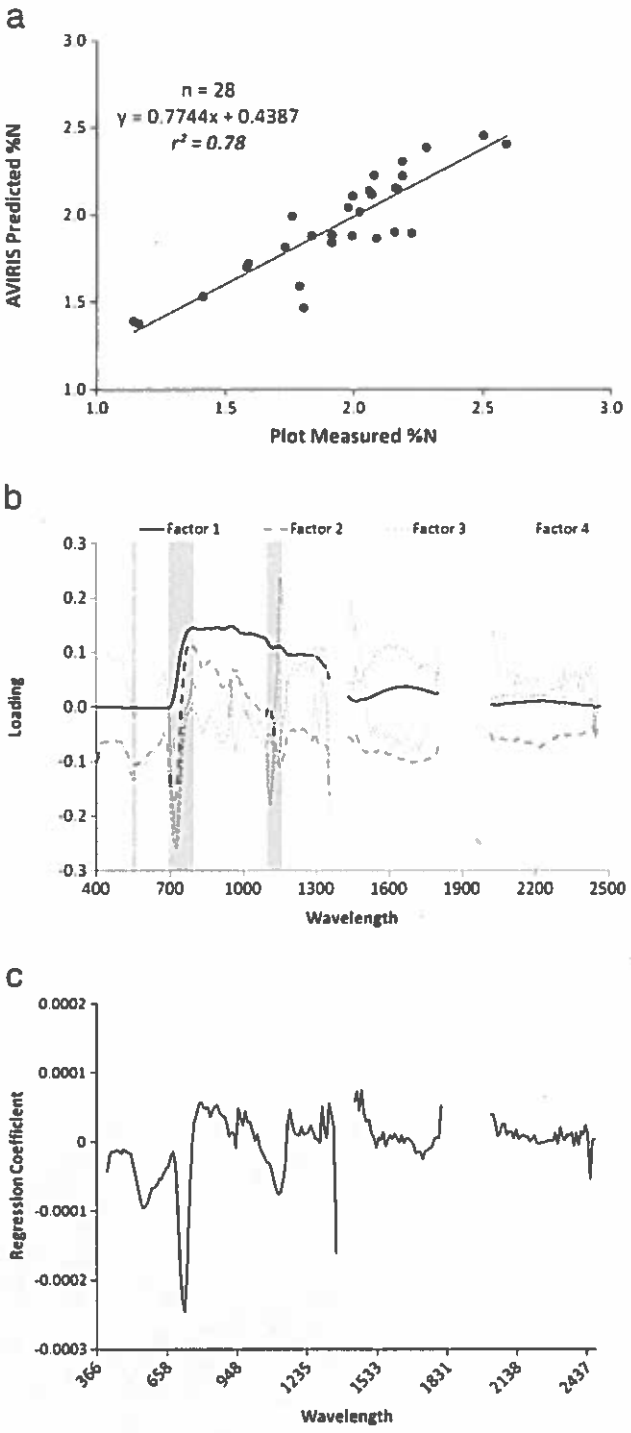

Fig. 5. Results from the PLS regression between plot-measured canopy N and AVIRIS reflectance values. (a) The relationship between plot-measured canopy N values and AVIRIS-predicted canopy N values, (b) the factor loadings describing individual band contributions from each of the four factors used in the PLS regression, and (c) the PLS regression coefficients used in the calculation of canopy N from AVIRIS imagery.

3.2. Cumulative disturbance impacts on forest structure

The results from our regression analyses suggest that cumulative disturbance has a negative effect on percent canopy cover (Fig. 8, Table 4). Canopy cover has a significant relationship with the cumulative DI map ($r^2 = 0.34$), but does not have any significant relationship with the most recent ΔDI images, indicating that percent canopy

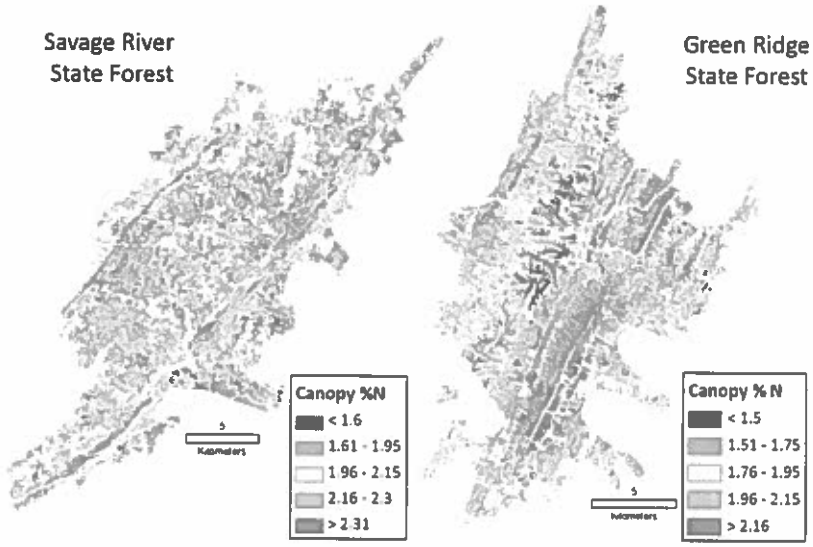

Fig. 6. AVIRIS-derived canopy N maps for both study areas. Non-forested land cover and clouds are masked.

cover may be a product of the additive impacts of past and present disturbances together, and not indicative of current disturbance status. When we analyzed the two study areas separately, the relationship remains significant with increasing strength ($r^2 = 0.66$ and $r^2 = 0.67$ for GRSF and SRSF, respectively).

3.3. Canopy N maps

The four-factor PLS model accounts for about 78% of the variability in plot-level measured canopy N (Fig. 5a) and about 63% of the variability in the AVIRIS reflectance spectra (data not shown). Root mean square error (RMSE) is 0.16%N, which is low relative to the mean canopy N of 2.0%N. The band loadings for each PLS latent factor describe the influential bands and can provide insight into the physical basis for spectroscopic detection of N. The first latent factor accounts for 92% of the explained variability in the AVIRIS spectra and resembled the general reflectance curve seen in vegetation (Fig. 5b). The remaining factors emphasize many absorption features that correspond with important leaf biochemical properties, such as chlorophyll and N-containing proteins. These absorption features are found in factor two at 560 nm, 1130 nm, and 1350 nm; in factor three at 560 nm, 1140 nm, and 2436 nm; and in factor four at 560 nm, 1150 nm, 1353 nm, 1442 nm, 2067 nm, and 2446 nm (Fig. 5b). Examination of the loadings also reveals influential bands within the "red edge". The relationship between plot-measured canopy N and AVIRIS canopy N is slightly less than unity ($y = 0.774x + 0.4387$), indicating

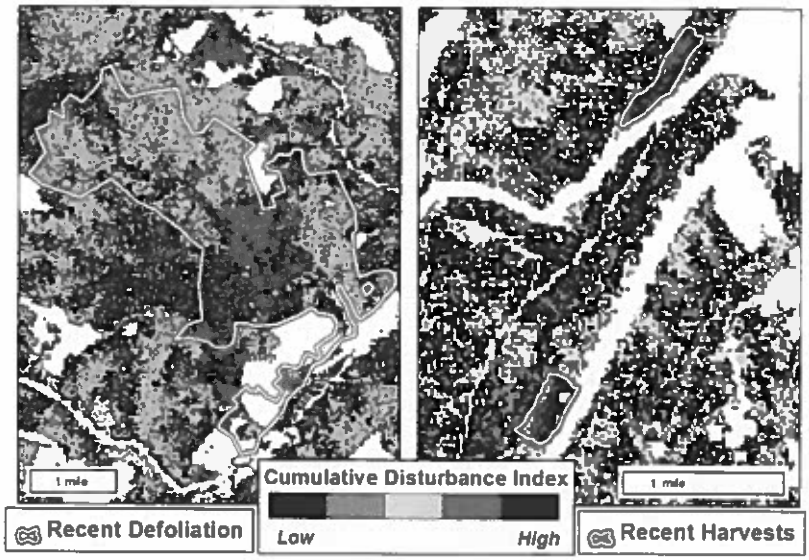

Fig. 7. Example visual assessment of the cumulative DI compared with GIS polygon data describing recent gypsy moth defoliation (since 2007) within SRSF and recent forest harvest (since 2000) disturbances within GRSF. Non-forested land cover and clouds are masked. Consistent with the known spatial patterns of the distinct disturbance agents, the cumulative disturbance map: (a) shows variable levels of disturbance intensity within areas of known defoliation (left panel), (b) shows abrupt areas of high disturbance intensity in forest harvest areas (right panel), and (c) generally shows minimal disturbance (green pixels) outside of areas designated by ancillary GIS polygon data on forest harvest or defoliation. In the case of SRSF, the recent defoliation event in 2007 was so extensive that the majority of forested land was affected. This is extensive defoliation event is evident in the cumulative DI.

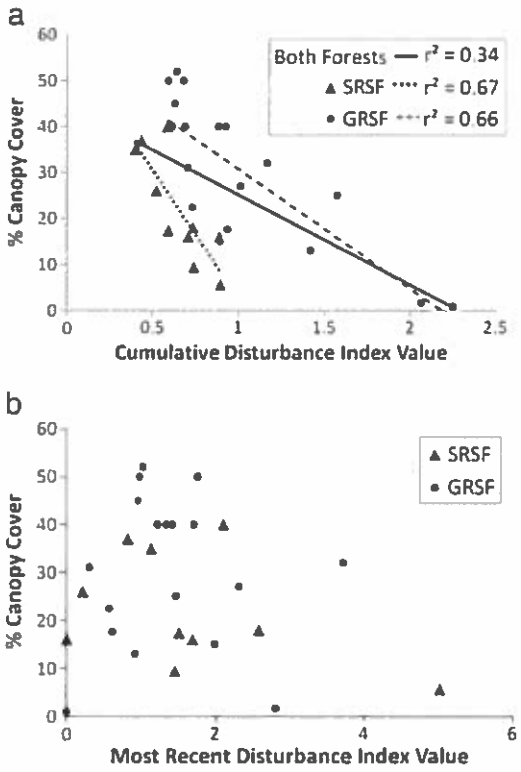

Fig. 8. The relationship between plot-measured percent canopy cover and (a) cumulative DI, and (b) the most recent ΔDI. The cumulative DI produced a strong relationship with % canopy cover. Results displayed are significant to the 0.01 level. N.S. refers to non-significant results.

that the dynamic range of the AVIRIS canopy N values is lower than that of the plot-measured canopy N values (Fig. 5a). This could introduce some error into our analysis; because, relative to the field data, the AVIRIS-measurements may be a less sensitive measure of canopy N.

3.4. Cumulative disturbance impacts on canopy N

Regression analyses focusing on the plot-measured canopy N values display no significant relationship with cumulative disturbance (Table 5). However, the watershed-scale relationships between canopy N and cumulative disturbance are significant and much stronger, but vary by study area (Fig. 9, Table 5). The strongest relationship occurs at SRSF ($r^2 = 0.57$), indicating that accumulated disturbances control over half of the spatial variability in canopy N during our study year (2009) at SRSF. Using the cumulative DI to assess watershed-scale variability in canopy N at GRSF produces a less strong, yet still significant, relationship ($r^2 = 0.40$). When considered together, the overall relationship for both forests holds ($r^2 = 0.54$).

Table 4
Results from the regressions (r^2) between % canopy cover and the two versions of DI. Non-significant results are indicated by ns. Results significant at the 0.01 level are displayed in bold. Results significant to the 0.001 level are displayed in bold and italics.

		GRSF	SRSF	Both forests
% Canopy cover	Cumulative DI	***0.66***	**0.67**	***0.34***
	Most recent ΔDI	ns	ns	ns

Table 5
Results from the regressions (r^2) between canopy % N values at the plot- and watershed-scale and the different versions of DI. Non-significant results are indicated by ns. Results significant to the 0.05 level are displaying in plain text. Results significant to the 0.001 level are displayed in bold.

		GRSF	SRSF	Both forests
Plot-level %N	Cumulative DI	ns	ns	ns
	Most recent ΔDI	0.30	ns	ns
Watershed-level %N	Cumulative DI	**0.40**	**0.57**	**0.54**
	Most recent ΔDI	ns	0.18	ns

4. Discussion

4.1. Cumulative disturbance index

The cumulative DI produces relatively strong relationships with percent canopy cover at the plot-level and with canopy percent N at the watershed-level. These results, combined with previous research on the additive nature of disturbances (Foster et al., 2003; Goodale & Aber, 2001; Latty et al., 2004; Pan et al., 2011) provide evidence for the utility of a cumulative method for assessing disturbance impacts on forest functioning. The cumulative disturbance index we have proposed represents a method for reconstructing a forest's accumulated disturbance history without the need for exhaustive, long-term field data collection, which is often unavailable or inconsistent (Cohen et al., 2010; Kennedy et al., 2010). Using an exponential weighting scheme, the model acknowledges years passed between image dates and accounts for them in the weighting factors, which can be important because yearly images are not always available due to cloud cover or other issues.

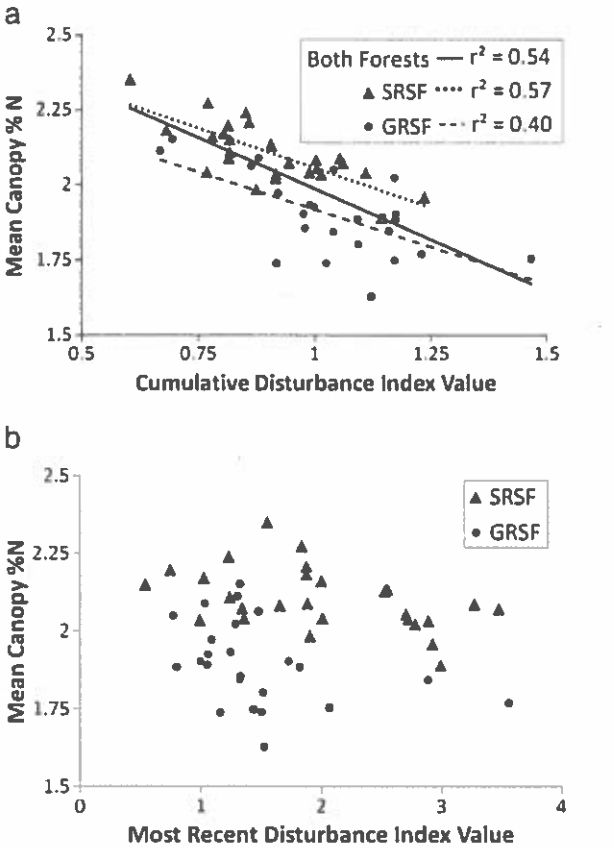

Fig. 9. The watershed-scale relationships between % canopy N and (a) cumulative DI, and (b) the most recent ΔDI. The cumulative DI produced a strong relationship with % canopy N. All displayed regression lines are significant at the 0.05 level.

Building off work using Landsat time series stacks on temporal trajectories of forest disturbance (Kennedy et al., 2007), two recent companion papers by Kennedy et al. (2010) and Cohen et al. (2010) describe Landtrendr, an algorithm designed to capture both disturbance trends and events in forests, and TimeSync, a visualization and data collection tool designed for use in validating change algorithms (such as Landtrendr). Huang et al. (2010) used an automated approach, the vegetation change tracker (VCT), to distinguish forest land cover types, mask clouds and water bodies, and map disturbances using Landsat time series stacks. Further developing these types of methods will prove invaluable now that the entire Landsat archive is available online for free download (Landsat Science Team, 2008). Our cumulative disturbance index may provide an additional component for use in these types of algorithms, creating more comprehensive and biophysically relevant measures of forest disturbance history.

Since a long-term, fine-grained, and spatially-extensive record of disturbance is not currently available for our study area (and, indeed, would be extremely rare for any forest), a traditional error matrix-approach to validating cumulative disturbance is not feasible. Nevertheless, our approach to mapping cumulative disturbance with the DI is validated in three ways. First, Healey et al. (2005) quantitatively assessed the accuracy of DI by creating 50 iterations of a comprehensive error matrix comparing DI with manually digitized reference maps. Subsequent studies have since used the DI (DeRose et al., 2011; Eshleman et al., 2009; Hais et al., 2009) to map disturbance in both conifer forests and eastern deciduous forests. Second, our visual assessments of the cumulative disturbance maps using coarse-grained, ancillary GIS data showed that our cumulative disturbance maps realistically reflect known patterns of disturbances that occurred throughout the study period (Fig. 7). Finally, the strong relationships with canopy cover (Fig. 8) and canopy N (Fig. 9) demonstrate that the cumulative disturbance index successfully captures biophysically-meaningful patterns in forest functioning.

One limitation of the cumulative DI approach is that not every year provides a cloud-free image, and in some instances, missing years may be critical in reconstructing a site's disturbance history. For example, the image for 22 August 2000 over GRSF contained more clouds than most of the other images used in this analysis; so as a test analysis, we created one cumulative DI that included this image and one that did not. GRSF experienced a major gypsy moth defoliation during this year, and the differences between our results suggest this disturbance event was important to the cumulative DI. The watershed-scale relationship between the weighted cumulative DI and canopy percent N at GRSF went from being a non-significant r^2 of 0.10 without the inclusion of the 2000 image to a significant r^2 of 0.40 with the inclusion of the 2000 image.

The implications of this test analysis are that the effectiveness of the cumulative DI is contingent on the availability of data. The relationships we observed in this analysis were significant, even though some years of imagery could not be included due to persistent cloud cover, so it is very possible that the relationship could become stronger with the inclusion of a full and complete set of input imagery. There are several ways around this limitation. Image compositing (Helmer & Ruefenacht, 2005; Roy et al., 2010) is a standard method for dealing with extensive cloud cover. Another option is to map cumulative disturbances with higher temporal resolution sensor (e.g. MODIS), especially as the data record accumulates from sensors like MODIS. Newly developed algorithms, such as Landtrendr (Kennedy et al., 2010) and VCT (Huang et al., 2010; Thomas et al., 2011), could also be used in future applications because they contain built-in, automated methods for masking out or avoiding cloud cover.

The use of a DI_{min} image for comparison in calculating forest disturbance across multiple dates of imagery builds off and expands upon previous work using ΔDI calculated from previous image years (Fig. 4). Eshleman et al. (2009) used ΔDI and synoptic water quality data to identify forest disturbance in a single watershed within Green Ridge State Forest. They found a strong linear relationship between ΔDI value and streamwater export of nitrate, providing validation and lending support for the use of ΔDI as a reliable indicator of disturbance intensity across broad scales. The advantage of the DI_{min} is that it alleviates the need to find a suitable reference year for comparison in change and disturbance detection. Though some level of reference could potentially be achieved using the Landsat images themselves (Cohen et al., 2010; Thomas et al., 2011), the DI_{min} provides an alternative approach to finding a suitable reference image for quantifying relative disturbance and change over a large temporal period.

Future studies that wish to make use of the cumulative disturbance index may also benefit from exploring other methods of weighting, such as other nonlinear weighting schemes. The independent variable under consideration may also dictate the weighting scheme selected. For example, forest structure and biomass often recover at a more rapid pace than nutrient availability (Bormann & Likens, 1979, Likens et al., 1978, Vitousek & Reiners, 1975). While much work has been done on disturbance mapping and disturbance dynamics, relatively little is known about the temporal trajectory of recovery. Thus, further exploratory work on such a trajectory would enhance the accuracy and value of the cumulative disturbance index. For example, the forest disturbance dynamics explored by Kennedy et al. (2007) and Huang et al. (2009, 2010) could be incorporated into future work to create weighting schemes based on observed spectral changes over dense stacks of Landsat imagery, which may result in more comprehensive cumulative disturbance indices (e.g., Helmer et al., 2011; Li et al., 2011).

4.2. Cumulative disturbance and forest structure

Our results support the idea that disturbances have a cumulative effect on forest structure. However, the differences between the study areas in the relationship between cumulative disturbance and forest structure (Fig. 8, Table 4) suggest that between-site differences may be quite large and have the potential to weaken the relationship when combining too many sites across different environmental gradients. In our study, these within-site differences are likely due to the differing species compositions of the two study sites. For example, GRSF is composed largely of oak species, while SRSF has oaks as well as northern hardwood and pine forest types. The diversity of species at SRSF likely results in differing vulnerabilities and responses to disturbance (Garnier et al., 2004; Peterson, 2007), which could have affected the slope and intercept of the relationship between cumulative DI and canopy cover. For this reason, it may be appropriate to include species type as a secondary independent variable in a multiple regression equation for analyses designed to assess multiple forest types.

The relationship between canopy cover and cumulative disturbance contains implications about the continued ability of a forest to sequester carbon after multiple years of compounding disturbance events. The relative lack of explanatory power provided by using the most recent ΔDI image compared with using the cumulative disturbance index suggests that the spatial variability in forest structure is affected by long-term successional dynamics (Kardol, Todd, Hanson, & Mulholland, 2010), and that studies assessing drivers of variability in forest structure, carbon stocks, and carbon fluxes should consider the additive effects of many previous disturbances.

4.3. Cumulative disturbance and canopy N

The PLS regressions using spectra from the AVIRIS images produced strong predictive relationships of canopy N (Fig. 5), and are comparable with calibration relationships produced from previous studies (e.g. Martin et al., 2008, McNeil et al., 2008, Smith et al.,

2002, Townsend et al., 2003). In general, SRSF displays higher canopy N values than GRSF, which could be a result of the differences in species composition. Species composition also may have affected the model accuracy. While similar species can be found at both study areas, the greater representation of field plots within the less species diverse GRSF forest (18 plots versus 10 plots at SRSF) may have influenced the ability of the model to predict canopy N across both regions. Nevertheless, the ability to directly map canopy N across the study areas proved to be essential for detecting the expected negative impact of cumulative disturbance on canopy N. Specifically, the AVIRIS-derived canopy N maps enabled us to average across local variability in canopy N, and find a robust signal of cumulative disturbance within the watershed-averaged values of canopy N. The localized variability confounding a significant relationship between field plot-measured canopy N and cumulative disturbance is likely caused by species composition. In eastern North American forests, species composition can explain up to 93% of the spatial pattern in canopy N (McNeil et al., 2008). This impact of species composition occurs from differences in the relative abundances of species with inherent differences in foliar N (McNeil et al., 2008; Wright et al., 2004), as well as the community-level impacts resulting from interactions among species with differing resource and N cycling strategies (Hobbie et al., 2006; Lovett, Weathers, Arthur, & Shultz, 2004; McNeil, Read, & Driscoll, 2012).

In our study, visual inspections of the canopy N maps suggest that different factors are driving the spatial patterns of canopy N to differing degrees in each forest. SRSF has been affected by several recent years of intense and widespread gypsy moth defoliation, and the stronger relationship between cumulative disturbance and canopy N reflects the idea that this most recent disturbance may be a strong control on canopy N in SRSF. The relationship with cumulative disturbance was less strong at GRSF, indicating that canopy N may be more strongly controlled by species composition. For example, low values of canopy N appear to follow a lower elevation band of white oak stands found in GRSF (Fig. 6, Foster & Townsend, 2004). Even within areas with good, stand-level species composition maps (as in our study area — see Foster & Townsend, 2004 and related unpublished maps at SRSF), running separate analyses for each species type found in the study areas proves to be overly complex. Hence, we suggest that quantitative measures of species composition are needed as an alternative to running parallel stand-level analyses. In particular, we suggest that measuring species by a continuous variable describing their canopy N responsiveness to disturbances could be incorporated as a secondary variable in a multiple regression equation and possibly improve the relationship between canopy percent N and cumulative DI.

In sum, while our results demonstrate a need to incorporate fine-scale drivers of variability in N status such as species composition, we have shown that field observations of the cumulative influence of disturbances on N status (Foster et al., 2003; Goodale & Aber, 2001; Latty et al., 2004) can be extended to a broader observational scale using remotely sensed imagery. In addition to studies of N status, we suggest that our approach for mapping cumulative disturbances may also lend itself to future studies on other biogeochemical processes (e.g. watershed-level retention of N and cations) that may be affected by the accumulating effects of disturbance across multiple years.

5. Conclusions

The cumulative DI produces significant relationships with percent canopy cover at the plot-level and with canopy percent N at the watershed-level. These results, combined with previous research on the additive nature of disturbances (Foster et al., 2003; Goodale & Aber, 2001; Latty et al., 2004; Pan et al., 2011) provide evidence for the utility of a cumulative method for assessing disturbance impacts on forest functioning. Our results support our two original hypotheses on the relationship of cumulative disturbance to canopy N and forest structure. Namely, we found that an increase in cumulative disturbance was associated with a decrease in both canopy N and forest canopy cover. Moreover, our study provided insights into the nature of disturbance as it accumulates over time and contributes to a growing literature on the temporal properties of forest disturbance dynamics. The cumulative DI consistently produced significant relationships at the watershed scale, suggesting that past disturbances do diminish over time but still influence the current condition of a forest. Using only the most current ΔDI maps consistently produced weaker, non-significant relationships, suggesting that current imagery alone may not be adequate to describe the disturbance legacies present in eastern forests. Thus, by detailing an approach for mapping the cumulative impact of disturbances and demonstrating the biophysical relevance of this approach in predicting current spatial patterns of canopy cover and canopy N, our study provides a useful step toward better understanding the long-term impacts of disturbances on forest processes and functions.

Acknowledgments

We thank B. Breslow, C. Parana, C. Leibfried, J. Griffith, and the foresters at GRSF and SRSF for field assistance and logistical support, as well as B. Peterjohn and T. Warner for comments on earlier versions of this manuscript. We appreciate generous financial support from West Virginia University, the NASA West Virginia Space Grant Consortium, the NASA Applied Sciences Program (grant #NNX09AO15G), and the NASA Terrestrial Ecology Program (grant #NNX08AN31G).

Author contributions: LND and BEM designed the fieldwork and image analyses; LND led the fieldwork, performed the image analyses, and wrote the paper with BEM; PGC, SPS, AS, KNE, and PAT contributed novel analytical methods and essential logistical support. All authors edited the final manuscript.

References

Aber, J. D. (1979). A method for estimating foliage-height profiles in broad-leaved forests. *The Journal of Ecology, 67*, 35–40.

Aber, J. D., McDowell, W. H., Nadelhoffer, K. J., Magill, A. H., Berntson, G., Kamekea, M., et al. (1998). Nitrogen saturation in temperate forest ecosystems: Hypotheses revisited. *BioScience, 48*, 921–934.

Asner, G. P. (1998). Biophysical and biochemical sources of variability in canopy reflectance. *Remote Sensing of Environment, 64*, 234–253.

Beck, D. E., & Hooper, R. M. (1986). Development of a Southern Appalachian hardwood stand after clearcutting. *Southern Journal of Appalachian Forestry, 10*, 168–172.

Bormann, F. H., & Likens, G. E. (1979). *Pattern and process in a forested ecosystem: Disturbance, development, and the steady state based on the Hubbard Brook ecosystem study*. New York: Springer-Verlag.

Chandler, G., Markham, B. L., & Helder, D. L. (2009). Summary of current radiometric calibration coefficients for Landsat MSS, TM, ETM+, and EO-1 ALI sensors. *Remote Sensing of Environment, 113*, 893–903.

Chapin, F. S., III, Matson, P. A., & Mooney, H. A. (2002). *Principles of terrestrial ecosystem ecology*. New York: Springer-Verlag.

Chapman, S. K., Langely, J. A., Hart, S. C., & Koch, G. W. (2006). Plants actively control nitrogen cycling: uncorking the microbial bottleneck. *New Phytologist, 169*, 27–34.

Chavez, P. (1996). Image-based atmospheric corrections — Revisited and improved. *Photogrammetric Engineering and Remote Sensing, 62*, 1025–1036.

Cohen, W. B., Yang, Z., & Kennedy, R. (2010). Detecting trends in forest disturbance and recovery using yearly Landsat time series: 2. TimeSync — Tools for calibration and validation. *Remote Sensing of Environment, 114*, 2911–2924.

DeRose, R. J., Long, J. N., & Ramsey, D. (2011). Combining dendrochronological data and the disturbance index to assess Engelmann spruce mortality caused by a spruce beetle outbreak in southern Utah, USA. *Remote Sensing of Environment, 115*, 2342–2349.

Driscoll, C. T., Whitall, D., Aber, J., Boyer, E., Castro, M., Cronan, C., et al. (2003). Nitrogen pollution in the northeastern United States: Sources, effects, and management options. *BioScience, 53*, 357–374.

Eshleman, K. N., McNeil, B. E., & Townsend, P. A. (2009). Validation of a remote sensing based index of forest disturbance using streamwater nitrogen data. *Ecological Indicators, 9*, 476–484.

Eshleman, K. N., Morgan, R. P., II, Webb, J. R., Deviney, F. A., & Galloway, J. N. (1998). Temporal patterns of nitrogen leakage from mid-Appalachian forested watersheds: Role of insect defoliation. *Water Resources Research, 34*, 2005–2016.

Evans, J. R. (1989). Photosynthesis and nitrogen relationships in leaves of C_3 plants. *Oecologia, 78*, 9–19.

Foster, D. R., Swanson, F., Aber, J. D., Burke, I., Brokaw, N., Tilman, D., et al. (2003). The importance of land-use legacies to ecology and conservation. *BioScience, 53*, 77–88.

Foster, J. R., & Townsend, P. A. (2004). Linking hyperspectral imagery and forest inventories for forest assessment in the Central Appalachians. *Proceedings of the 14th Central Hardwood Conference. USDA Forest Service General Technical Report* March 17 – 19, 2004.

Galloway, J. N., Townsend, A. R., Erisman, J. W., Bekunda, M., Cai, Z., Freney, J. R., et al. (2008). Transformation of the nitrogen cycle: Recent trends, questions, and potential solutions. *Science, 320*, 889–892.

Garnier, E., Cortez, J., Billes, G., Navas, M. -L., Roumet, C., Debussche, M., et al. (2004). Plant functional markers capture ecosystem properties during secondary succession. *Ecology, 85*, 2630–2637.

Garnier, E., Shipley, B., Roumet, C., & Laurent, G. (2001). A standardized protocol for the determination of specific leaf area and leaf dry matter content. *Functional Ecology, 15*, 688–695.

Goodale, C. L., & Aber, J. D. (2001). The long-term effects of land-use history on nitrogen cycling in northern hardwood forests. *Ecological Applications, 11*, 253–267.

Goodwin, N. R., Coops, N. C., Wulder, M. A., & Gillanders, S. (2008). Estimation of insect infestation dynamics using a temporal sequence of Landsat data. *Remote Sensing of Environment, 12*, 3680–3689.

Green, R. O., Eastwood, M. L., Sartare, C. M., Chrien, T. G., Aronsson, M., Chippendale, B. J., et al. (1998). Imaging spectroscopy and the Airborne Visible Infrared Imaging Spectrometer (AVIRIS). *Remote Sensing of Environment, 65*, 227–248.

Hais, M., Jonasova, M., Langhammer, J., & Kucera, T. (2009). Comparison of two types of forest disturbance using multitemporal Landsat TM/ETM+ imagery and field vegetation data. *Remote Sensing of Environment, 113*, 835–845.

Haynes, K. J., Liebhold, A. M., & Johnson, D. M. (2009). Spatial analysis of harmonic oscillation of gypsy moth outbreak intensity. *Oecologia, 159*, 249–256.

Healey, S. P., Cohen, W. B., Zhiqiang, Y., & Krankina, O. N. (2005). Comparison of Tasseled-Cap Landsat data structures for use in forest disturbance detection. *Remote Sensing of Environment, 97*, 301–310.

Helmer, E. H., & Ruefenacht, B. (2005). Cloud-free satellite image mosaics with regression trees and histogram matching. *Photogrammetric Engineering and Remote Sensing, 71*, 1079–1089.

Helmer, E. H., Ruzycki, T. S., Wunderle, J. M., Vogesser, S., Ruefenacht, B., Kwit, C., et al. (2011). Mapping tropical dry forest height, foliage height profiles and disturbance type and age with a time series of cloud-cleared Landsat and ALI image mosaics to characterize avian habitat. *Remote Sensing of Environment, 114*, 2457–2473.

Hobbie, S. E., Reich, P. B., Oleksyn, J., Ogdahl, M., Zytkowiak, R., Hale, C., et al. (2006). Tree species effects on decomposition and forest floor dynamics in a common garden. *Ecology, 87*, 2288–2297.

Huang, C., Goward, S. N., Masek, J. G., Thomas, N., Zhu, Z., & Vogelmann, J. E. (2010). An automated approach for reconstructing recent forest disturbance history using dense Landsat time series stacks. *Remote Sensing of Environment, 114*, 183–198.

Huang, C., Goward, S. N., Schleeweis, K., Thomas, N., Masek, J. G., & Zhu, Z. (2009). Dynamics of national forests assessed using the Landsat record: Case studies in eastern United States. *Remote Sensing of Environment, 113*, 1430–1442.

Jin, S., & Sader, S. A. (2005). Comparison of time series tasseled cap wetness and the normalized different moisture index in detecting forest disturbance. *Remote Sensing of Environment, 94*, 364–372.

Johnson, D. M., Liebhold, A. M., & Bjørnstad, O. N. (2006). Geographical variation in the periodicity of gypsy moth outbreaks. *Ecography, 29*, 367–374.

Kardol, P., Todd, D. E., Hanson, P. J., & Mulholland, P. J. (2010). Long-term successional forest dynamics: species and community responses to climatic variability. *Journal of Vegetation Science, 21*, 627–642.

Kennedy, R. E., Cohen, W. B., & Schroeder, T. A. (2007). Trajectory-based change detection for automated characterization of forest disturbance dynamics. *Remote Sensing of Environment, 110*, 370–386.

Kennedy, R. E., Yang, Z., & Cohen, W. B. (2010). Detecting trends in forest disturbance and recovery using yearly Landsat time series: 1. LandTrendr – Temporal segmentation algorithms. *Remote Sensing of Environment, 114*, 2897–2910.

Kokaly, R. F. (2001). Investigating a physical basis for spectroscopic estimates of leaf nitrogen concentration. *Remote Sensing of Environment, 75*, 153–161.

Landsat Science Team (C.E. Woodcock, R. Allen, M. Anderson, A. Belward, R. Bindschadler, W.B. Cohen, F. Gao, S.N. Goward, D. Helder, E. Helmer, R. Nemani, L. Orepoulos, J. Schott, P. Thenkbail, E. Vermote, J. Vogelmann, M. Wulder, R. Wynne). (2008). Free access to Landsat data. Letter, *Science, 320*, 1011.

Latty, E. F., Canham, C. D., & Marks, P. L. (2004). The effects of land-use history on soil properties and nutrient dynamics in northern hardwood forests of the Adirondack Mountains. *Ecosystems, 7*, 193–207.

LeBauer, D. S., & Treseder, K. K. (2008). Nitrogen limitation of net primary productivity in terrestrial ecosystems is globally distributed. *Ecology, 89*, 371–379.

Li, A., Huang, C., Sun, G., Shi, H., Toney, C., Zhu, Z., et al. (2011). Modeling the growth of young forests regenerating from recent disturbances in Mississippi using Landsat time series observations and ICESat/GLAS lidar data. *Remote Sensing of Environment, 115*, 1837–1849.

Likens, G. E., Bormann, F. H., Johnson, N. M., Fisher, D. W., & Pierce, R. S. (1970). Effects of forest cutting and herbicide treatment on nutrient budgets in the Hubbard Brook Watershed-Ecosystem. *Ecological Monographs, 40*, 23–47.

Likens, G. E., Bormann, F. H., Pierce, R. S., & Reiners, W. A. (1978). Recovery of a deforested ecosystem. *Science, 199*, 492–496.

Lovett, G. M., Weathers, K. C., Arthur, M. A., & Shultz, J. C. (2004). Nitrogen cycling in a northern hardwood forest: Do species matter? *Biogeochemistry, 67*, 289–308.

MacArthur, R. H., & Horn, H. S. (1969). Foliage profile by vertical measurements. *Ecology, 50*, 802–804.

Malczewski, J. (1999). *GIS and MultiCriteria Decision Analysis*. New York: John Wiley & Sons, Inc.

Martin, M. E., & Aber, J. D. (1997). High spectral resolution remote sensing of forest canopy lignin, nitrogen, and ecosystem processes. *Ecological Applications, 7*, 431–443.

Martin, M. E., Plourde, L. C., Ollinger, S. V., Smith, M. -L., & McNeil, B. E. (2008). A generalizable method for remote sensing of canopy nitrogen across a wide range of forest ecosystems. *Remote Sensing of Environment, 112*, 3511–3519.

Mash, J. (1996). *The Land of the living*. Cumberland: Commercial Press.

McNeil, B. E., de Beurs, K. M., Eshleman, K. N., Foster, J. R., & Townsend, P. A. (2007). Maintenance of ecosystem nitrogen limitation by ephemeral forest disturbance: An assessment using MODIS, Hyperion, and Landsat ETM+. *Geophysical Research Letters, 34*, L19406, doi:10.1029/2007GL031387.

McNeil, B. E., Read, J. M., & Driscoll, C. T. (2012). Foliar nitrogen responses to the environmental gradient matrix of the Adirondack Park, New York. *Annals of the Association of American Geographers, 102*, 1–15.

McNeil, B. E., Read, J. M., Sullivan, T. J., McDonnell, T. C., Fernandez, I. J., & Driscoll, C. T. (2008). The spatial pattern of nitrogen cycling in the Adirondack Park, New York. *Ecological Applications, 18*, 438–452.

Ollinger, S. V., Richardson, A. D., Martin, M. E., Hollinger, D. Y., Frolking, S. E., Reich, P. B., et al. (2009). Canopy nitrogen, carbon assimilation, and albedo in temperate and boreal forests: functional relations and potential climate feedbacks. *Proceedings of the National Academy of Sciences, 105*, 19335–19340.

Ollinger, S. V., & Smith, M. L. (2005). Net primary production and canopy nitrogen in a temperate forest landscape: An analysis using imaging spectroscopy, modeling and field data. *Ecosystems, 8*, 760–778.

Pan, Y., Chen, J. M., Birdsey, R., McCullough, He, L., & Deng, F. (2011). Age structure and disturbance legacy of North American forests. *Biogeosciences, 8*, 715–732.

Pan, Y., Hom, J., Jenkins, J., & Birdsey, R. (2004). Importance of foliar nitrogen concentration to predict forest productivity in the Mid-Atlantic region. *Forest Science, 50*, 279–289.

Peterson, C. J. (2007). Consistent influence of tree diameter and species on damage in nine eastern North America tornado blowdowns. *Forest Ecology and Management, 250*, 96–108.

Roy, D. P., Ju, J. C., Kline, K., Scaramuzza, P. L., Kovalskyy, V., Hansen, M., et al. (2010). Web-enabled Landsat Data (WELD): Landsat ETM plus composited mosaics of the conterminous United States. *Remote Sensing of Environment, 114*, 35–49.

Sader, S. A., & Legaard, K. R. (2008). Inclusion of forest harvest legacies, forest type, and regeneration spatial patterns in updated forest maps: A comparison of mapping results. *Forest Ecology and Management, 255*, 3846–3856.

Schaefer, W. D., & Brown, T. C. (1991). *Ten year resource management plan: Savage River State Forest: Draft document*. State of Maryland, Department of Natural Resources, Public Lands Administration, State Forest & Park Service.

Smith, M. -L., & Martin, M. E. (2001). A plot-based method for rapid estimation of forest canopy chemistry. *Canadian Journal of Forest Research, 31*, 549–555.

Smith, M. -L., Martin, M. E., Ollinger, S. V., & Plourde, L. (2003). Analysis of hyperspectral data for estimation of temperate forest canopy nitrogen concentration: Comparison between an airborne (AVIRIS) and a spaceborne (Hyperion) sensor. *EEE Transactions on Geosciences and Remote Sensing, 41*, 1332–1337.

Smith, M. -L., Ollinger, S. V., Martin, M. E., Aber, J. D., Hallett, R. A., & Goodale, C. L. (2002). Direct estimation of aboveground forest productivity through hyperspectral remote sensing of canopy nitrogen. *Ecological Applications, 12*, 1286–1302.

Thomas, N., Huang, C., Goward, S. N., Powell, S., Rishmawi, K., Schleeweis, K., et al. (2011). Validation of North American forest disturbance dynamics derived from Landsat time series stacks. *Remote Sensing of Environment, 115*, 19–32.

Townsend, P. A., Eshleman, K. N., & Welcker, C. (2004). Remote sensing of Gypsy moth defoliation to assess variations in stream nitrogen concentration. *Ecological Applications, 14*, 504–516.

Townsend, P. A., Foster, J. R., Chastain, R. A., & Currie, W. S. (2003). Application of imaging spectroscopy to mapping canopy nitrogen in the forests of the central Appalachian Mountains using Hyperion and AVIRIS. *IEEE Transactions on Geoscience and Remote Sensing, 41*, 1347–1354.

Vaieretti, M. V., Diaz, S., Vile, D., & Garnier, E. (2007). Two measurement methods of leaf dry matter content produce similar results in a broad range of species. *Annals of Botany, 99*, 955–958.

Vitousek, P. M., Gosz, J. R., Grier, C. C., Melillo, J. M., Reiners, W. A., & Todd, R. L. (1979). Nitrate losses from disturbed ecosystems. *Science, 204*, 469–474.

Vitousek, P. M., & Howarth, R. W. (1991). Nitrogen limitation on land and in the sea: How can it occur? *Biogeochemistry, 13*, 87–115.

Vitousek, P. M., & Reiners, W. A. (1975). Ecosystem succession and nutrient retention: A hypothesis. *BioScience, 25*, 376–381.

Vogelmann, J. E., Tolk, B., & Zhu, Z. (2009). Monitoring forest changes in the southwestern United States using multitemporal Landsat data. *Remote Sensing of Environment, 113*, 1739–1748.

Wessman, C. A., Aber, J. D., Peterson, D. L., & Melillo, J. M. (1988). Remote sensing of canopy chemistry and nitrogen cycling in temperate forest ecosystems. *Nature, 335*, 154–156.

Wright, I. J., Reich, P. B., Westoby, M., Ackerly, D. D., Baruch, Z., Bongers, F., et al. (2004). The worldwide leaf economics spectrum. *Nature, 428*, 821–827.